

Corner contribution to cluster numbers in the Potts model

István A. Kovács,^{1,2,*} Eren Metin Elçi,^{3,4,†} Martin Weigel,^{3,4,‡} and Ferenc Igloi^{1,2,§}

¹Wigner Research Centre, Institute for Solid State Physics and Optics, H-1525 Budapest, P.O.Box 49, Hungary

²Institute of Theoretical Physics, Szeged University, H-6720 Szeged, Hungary

³Applied Mathematics Research Centre, Coventry University, Coventry, CV1 5FB, United Kingdom

⁴Institut für Physik, Johannes Gutenberg-Universität Mainz, Staudinger Weg 7, D-55099 Mainz, Germany

(Received 22 November 2013; revised manuscript received 4 February 2014; published 24 February 2014)

For the two-dimensional Q -state Potts model at criticality, we consider Fortuin-Kasteleyn and spin clusters and study the average number N_Γ of clusters that intersect a given contour Γ . To leading order, N_Γ is proportional to the length of the curve. Additionally, however, there occur logarithmic contributions related to the corners of Γ . These are found to be universal and their size can be calculated employing techniques from conformal field theory. For the Fortuin-Kasteleyn clusters relevant to the thermal phase transition, we find agreement with these predictions from large-scale numerical simulations. For the spin clusters, on the other hand, the cluster numbers are not found to be consistent with the values obtained by analytic continuation, as conventionally assumed.

DOI: [10.1103/PhysRevB.89.064421](https://doi.org/10.1103/PhysRevB.89.064421)

PACS number(s): 64.60.De, 05.50.+q, 11.25.Hf, 64.60.an

I. INTRODUCTION

The Potts model [1], assigning a Q -state spin variable to each site of a lattice with distinct energy contributions between like and unlike spins, describes a rich set of phase ordering phenomena [2]. As special cases, it includes the simpler problem of (bond) percolation for $Q \rightarrow 1$ as well as the Ising model ($Q = 2$) [3]. While these phase transitions are continuous, for sufficiently large values of Q the transition becomes first order. In two dimensions, this occurs for $Q > 4$ [2]. While no exact solution is available for the case of general Q , a number of rigorous results regarding the transition temperatures and critical-point parameters are available from duality and mappings to vertex models [3]. Further results follow from the Coulomb gas mapping [4], conformal invariance [5], and more recently, the framework of Schramm-Loewner evolution (SLE) [6].

The relation between the Potts model and percolation [7] as a purely geometric phase transition becomes apparent from a transformation to a graph-theoretic problem introduced by Fortuin and Kasteleyn [8]. There, edges of the lattice are activated with probability p as in the percolation problem, but each configuration receives an additional weight proportional to $Q^{N_{\text{tot}}(F)}$, where $N_{\text{tot}}(F)$ is the number of connected components resulting from the bond configuration F . For the choice $p = p_{\text{FK}} = 1 - e^{-K}$, where K denotes the reduced coupling, the percolation transition coincides with the thermal transition of the Potts model and all magnetic observables can be related to geometric quantities in the percolation language [9,10], such that the fractal structure and connectivity properties of the Fortuin-Kasteleyn (FK) clusters encode the complete critical behavior.

One of the basic properties of such percolation configurations is the total number of clusters. To leading order, this is proportional to the size of the system. Additionally,

however, one expects corrections due to boundary effects resulting from the presence of surfaces, edges and corners. While, in general, such correction terms are nonuniversal, Cardy and Peschel showed that the corner contribution to the free energy of two-dimensional, conformally invariant systems is related to the central charge and hence universal [11]. To be specific, consider a contour Γ in the bulk. What is the number of clusters, N_Γ , which intersect Γ when Γ is large, but much smaller than the size of the system? Two of us have recently studied this problem in the percolation limit $Q \rightarrow 1$ and found a logarithmically divergent corner contribution to N_Γ [12]. Using conformal invariance and the Cardy-Peschel formula [11] allowed us to calculate this corner contribution analytically. Full consistency was found with extensive numerical simulations for a range of different 2D geometries. Here we investigate whether similar results hold for the more general case of the random-cluster model with arbitrary values of Q . We generalize the analytical calculations and confront the resulting predictions with large-scale numerical simulations for $Q = 1, 2, 3$, and 4, as well as the fractional value $Q = 0.5$.

Another type of geometrical object in the Potts model are the clusters of like spins that result from the Fortuin-Kasteleyn construction outlined above with the alternative choice $p = 1$. These also undergo a percolation transition but, in general, it does not occur at the thermal phase transition point. In two dimensions, however, both transitions coincide and analogous questions can be studied (such as fractal dimensions, connectivity properties, etc.) as for the FK clusters. It is found that, for a given Q , FK and spin clusters belong to conformal field theories of the same central charge [13]:

$$c = 1 - \frac{3(4-g)^2}{2g}, \quad (1)$$

where $g = g(Q)$ is the Coulomb gas parameter. Equation (1) has two solutions, g and g' , which are related as $gg' = 16$. For the FK clusters, g is given by the solution of

$$Q = 2 + 2 \cos(g\pi/2), \quad (2)$$

*kovacs.istvan@wigner.mta.hu

†elcie@uni.coventry.ac.uk

‡martin.weigel@coventry.ac.uk

§igloi.ferenc@wigner.mta.hu

with $2 \leq g \leq 4$. For the spin clusters, one should use $g' = 16/g$, resulting in $4 \leq g' \leq 8$ [14,15]. Here, $g' = \kappa$ is just the SLE parameter [16]. We note that in Eq. (2), the range $4 \leq g \leq 8$ represents the tricritical branch of the (annealed) site-diluted Potts model [17], in which the FK (spin) clusters are expected to be mapped to the spin (FK) clusters in the critical branch [18–20]. In general, results for the critical FK clusters are conjectured to be related to the critical spin clusters by analytical continuation, by making the substitution $g \rightarrow g'$. This type of analytical continuation appears to work well on the level of the fractal dimensions, as shown in a number of numerical investigations [14,15,21–24]. The universal prefactor in the area distribution of Ising spin clusters follows the above description as well [25]. More recently, however, the three-point connectivities were studied and the numerical results concerning the spin clusters disagree with the conjecture of analytical continuation [26]. In the context of corner contributions to the cluster numbers it is natural, then, to also study the behavior of spin clusters with $p = 1$ or, more generally, the behavior of the continuity of possible cluster definitions as the bond dilution parameter p is varied.

The rest of the paper is organized as follows. In Sec. II, we introduce the bond-diluted model and present the calculation of the corner contribution for FK clusters in the framework of the random-cluster representation and the arguments of conformal field theory following the work of Cardy and Peschel. The numerical results are presented in Sec. III. Finally, Sec. IV contains our conclusions.

II. CLUSTER NUMBERS IN THE POTTS MODEL

We consider the Q -state Potts model defined by the Hamiltonian [2]

$$\mathcal{H}/k_B T = -K \sum_{(i,j)} \delta_{s_i, s_j}, \quad (3)$$

with the Potts spin variables $s_i = 1, 2, \dots, Q$, where the summation is over nearest-neighbor pairs only. We restrict ourselves here to the model on the square lattice with a total of n sites and m bonds. Following the prescription introduced by Fortuin and Kasteleyn [8], the partition function of the model can be written as

$$Z(Q) \sim \sum_F Q^{N_{\text{tot}}(F)} p^{M(F)} (1-p)^{m-M(F)}, \quad (4)$$

where the bond configuration F consists of $N_{\text{tot}}(F)$ connected components and has a total of $M(F)$ active edges. Here the bond occupation probability between neighboring sites with the same Potts state is given by $p = p_{\text{FK}} = 1 - e^{-K}$, such that the clusters of F are FK clusters. In contrast to the Potts model of Eq. (3), which only makes sense for integer values of Q , the Fortuin-Kasteleyn form (4) is valid for arbitrary positive real Q . Regular bond percolation is easily seen to correspond to the limit $Q \rightarrow 1$. The mean total number of FK clusters is

$$\langle N_{\text{tot}} \rangle = Q \frac{\partial \ln Z(Q)}{\partial Q}. \quad (5)$$

Let us now introduce a contour Γ and assume for simplicity that Γ runs on top of a subset of the bonds. If we fix all spins on Γ (in state 1, say), but leave the couplings unchanged, the

partition function becomes

$$Z_\Gamma(Q) \sim \sum_F Q^{N_{\text{tot}}(F) - N_\Gamma} p^{M(F)} (1-p)^{m-M(F)}, \quad (6)$$

where N_Γ is the number of clusters which intersect Γ . As a result,

$$\langle N_{\text{tot}} - N_\Gamma \rangle = Q \frac{\partial \ln Z_\Gamma(Q)}{\partial Q}. \quad (7)$$

At the critical point, $e^{K_c} = 1 + \sqrt{Q}$ (see Ref. [2]), we can write [11,12]:

$$\ln Z(Q) \sim A f_b(Q), \quad (8)$$

$$\ln Z_\Gamma(Q) \sim A f_b(Q) + L_\Gamma f_s(Q) + C_\Gamma(Q) \ln L_\Gamma,$$

where $A \propto n$ is the total area, L_Γ is the length of Γ , and f_b and f_s are the bulk and surface free-energy densities, respectively. The latter are nonuniversal quantities. The last term in Eq. (8) represents the corner contribution. Together with Eqs. (5) and (7), we hence obtain

$$\langle N_\Gamma \rangle = -Q f'_s(Q) L_\Gamma + b_\Gamma(Q) \ln L_\Gamma, \quad (9)$$

with $b_\Gamma(Q) = -Q C'_\Gamma(Q)$. Analogous to the percolation case discussed in Ref. [12], we argue that the partition function $Z_\Gamma(Q)$ decomposes exactly into a product of the partition functions $Z_\Gamma^{\text{int}}(Q)$ for the interior of Γ , and $Z_\Gamma^{\text{ext}}(Q)$ for the exterior. If there were only clusters that do not cross Γ , this property was clearly fulfilled. Clusters with common points with the boundary, however, are all in the same Potts state, exactly as for percolation, thus including these does not violate the product property. Consequently, we can apply the Cardy-Peschel formula [11] both to the exterior boundary, with corners with interior angle γ_k , and to the interior boundary, with γ_k replaced by $2\pi - \gamma_k$. Using the results of Ref. [11], we therefore deduce that the prefactor of the logarithm in Eq. (8) is given by

$$C_\Gamma(Q) = \frac{c(Q)}{24} \sum_k \left[\left(\frac{\pi}{\gamma_k} \right) - \left(\frac{\gamma_k}{\pi} \right) + \left(\frac{\pi}{2\pi - \gamma_k} \right) - \left(\frac{2\pi - \gamma_k}{\pi} \right) \right], \quad (10)$$

where γ_k is the interior angle at each corner, and $c(Q)$ is the central charge as given in Eq. (1). Using the critical branch of Eq. (2), we have

$$Q c'(Q) \equiv \beta(Q) = \frac{3}{\pi} \frac{1 - 16/g^2}{\tan(\pi g/4)}, \quad (11)$$

thus

$$b_\Gamma(Q) = \beta(Q) A_\Gamma, \quad (12)$$

where A_Γ depends on the geometry of Γ , but does not depend on Q . We summarize the values of $\beta(Q)$ for the cases $Q = 0.5, 1, 2, 3$, and 4, studied numerically below in the last row of Table I.

In order to potentially extend these considerations to the case of spin clusters or, more generally, the case of arbitrary values of the dilution parameter p , we consider the Hamiltonian of the diluted Potts model [9,27,28]

$$\mathcal{H}_{\text{dil}}/k_B T = \mathcal{H}/k_B T - J \sum_{(i,j)} (\delta_{\tau_i, \tau_j} - 1) \delta_{s_i, s_j}, \quad (13)$$

TABLE I. Numerical estimates for the prefactor β of the corner contribution for the FK clusters using different contour geometries as compared to the conformal predictions of Eq. (11). The conformal predictions in the last row are $\frac{5\sqrt{3}}{4\pi}$, $\frac{7}{3\pi}$, $\frac{33\sqrt{3}}{25\pi}$, and $\frac{6}{\pi^2}$ for $Q = 1, 2, 3$, and 4, respectively.

Q	0.5	1	2	3	4
squares	0.589(10)	0.689(13)	0.742(9)	0.734(7)	0.669(27)
lines	0.598(34)	0.687(12)	0.739(11)	0.718(11)	0.632(4)
crosses	0.614(30)	0.692(2)	0.742(8)	0.730(3)	0.650(22)
CFT	0.5933	0.6892	0.7427	0.7278	0.6079

where $\tau_i = 1, 2, \dots, P$ is an auxiliary Potts variable, and we take the limit $P \rightarrow 1$. Here, in general, $p = 1 - e^{-J}$ is different from p_{FK} . As an analysis of the renormalization group flows shows [9], the critical surface of \mathcal{H}_{dil} is at $K = K_c$ and it contains two fixed points: the FK fixed point at $p = p_{\text{FK}}$, i.e., at $J = K_c$, is repulsive and controls the scaling of the critical FK clusters discussed above. The spin (or Potts) fixed point at $p = p_S > p_{\text{FK}}$, on the other hand, is attractive and controls the scaling behavior of the spin clusters. For the purposes of our study, therefore, it is natural to conjecture that the corner contribution to the spin cluster number is described by Eqs. (9)–(12), but using the analytical continuation $4 \leq g' \leq 8$ of Eqs. (1) and (2) corresponding to the value of Q under consideration. For the Ising model $Q = 2$, for instance, we have $c = 1/2$ with $g = 3$ and $g' = 16/3$, thus resulting in $\beta = 7/3\pi$ for the FK clusters and $\beta = 7\sqrt{3}/16\pi$ for the spin clusters, cf. the values collected in Tables I and II. In the next section, we shall check these predictions with numerical simulations.

III. NUMERICAL RESULTS

To test the relations for the corner contribution to the cluster numbers in the random-cluster model conjectured from conformal field theory, we performed numerical simulations for a number of different values of Q . All simulations were carried out at the critical point of square-lattice systems of edge length L . With the exception of the line segment at a free boundary discussed below in Sec. III A 4, we employed periodic boundary conditions. For the integer values $Q = 1, 2, 3$, and 4, our simulations were performed using the Swendsen-Wang algorithm [29]. For $Q = 0.5$, we used a recent implementation of Sweeny's single-bond method [30] based on a poly-logarithmic connectivity algorithm [31]. For

TABLE II. Numerical estimates for the prefactor β of the corner contribution for the spin clusters using different contour geometries as compared to the analytic continuation of the conformal predictions of Eq. (11).

Q	2	3	4
squares	0.480(6)	0.703(10)	0.796(24)
lines	0.486(10)	0.659(13)	0.653(5)
crosses	0.485(9)	0.662(14)	0.665(15)
CFT	$\frac{7\sqrt{3}}{16\pi} = 0.2412$	$\frac{11}{12\pi} \sqrt{1 + \frac{2\sqrt{3}}{5}} = 0.4016$	$\frac{6}{\pi^2} = 0.6079$

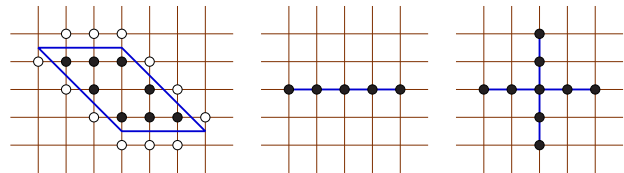


FIG. 1. (Color online) Shapes of the contours used in the calculation: sheared squares, line segments in the bulk, and crosses.

a range of system sizes $64 \leq L \leq 2048$, we thus generated at least 10^4 approximately independent configurational samples each. For integer Q , these spin configurations were subjected to an additional post-processing step, joining like spins with a probability p to form clusters including, in particular, the choice $p = 1$ corresponding to spin clusters. For $Q = 0.5$, it is not obvious how to construct an analog of spin configurations, such that we had to restrict our analysis to the FK clusters there. For each type of clusters, we then counted crossings with a number of different contours to be described next.

A. Shapes of the contours

With the cluster configurations at hand, we analyzed a number of different contours Γ , in particular (sheared) squares, line segments in the bulk and at a free boundary, as well as crosses. Three of these shapes are illustrated in Fig. 1. We calculated the corner contributions using the geometric approach introduced earlier [12,32]: for each sample, $\langle N_\Gamma \rangle$ is calculated in two geometries which have the same boundary term, but different corner contributions (often it is absent). Hence the difference of the two expression provides access to the corner contribution of the given sample. This approach is useful for cases where strong corrections in the boundary terms are present. For the $Q = 4$, Potts model studied here, where there are extra logarithmic corrections [33], this method spares us to disentangle these corrections from the logarithmic corner contribution.

1. Square and sheared squares

The first geometry considered here is a square of edge length $L/2$. As shown in detail in Ref. [32], the relevant corner contribution can be computed from comparing two arrangements of subdividing the system into squares or strips that have the same overall boundary, but the strip configuration has no corners. Hence the corner contribution can be found from the difference of the corresponding cluster numbers. Additionally, one can consider a sheared version of the square, having an opening angle $\gamma \leq \pi/2$ and both its base and its altitude are given by $L/2$. For this case, the angular dependence for the corner contribution is found to be

$$A_\Gamma = \frac{1}{12} \left[4 - \pi \left(\frac{1}{\gamma} + \frac{1}{\pi - \gamma} + \frac{1}{\pi + \gamma} + \frac{1}{2\pi - \gamma} \right) \right]. \quad (14)$$

For the sheared case, the contour Γ cannot run along a subset of the bonds. Instead, we allow it to have an arbitrary position and consider an inner and an outer layer of spins adjacent to the contour as illustrated in the left panel of Fig. 1. We then consider two types of crossing clusters. Type (a) clusters have

common points with sites of both layers, while type (*b*) clusters include all (*a*) clusters and also those that have common points with only one of the layers, however, with a weight of $1/2$. This latter case corresponds to N_Γ being averaged over the inner and outer layers. The asymptotic value of the prefactor of the corner contribution is the same for both type of clusters, but the finite-size corrections are found to be of different sign, which turns out to be useful for performing the finite-size extrapolations.

2. Line segments in the bulk

An even simpler geometry is given by a line segment located in the interior of the system, which has two exterior angles of each $\gamma = 2\pi$, so that $A_\Gamma = 1/8$. In the geometric approach the line is restricted to lie on top of a set of lattice points (see the middle panel of Fig. 1) and has a length of either $L/2$ or L . In the latter case (with periodic boundary conditions), there is evidently no corner contribution. In the former case, we take two consecutive segments and calculate N_Γ for each of them independently. In this way, the clusters that have common points with both segments are calculated twice when we compare them with the number of clusters for the contour of length L . Thus, in this case, the corner contribution for *one* segment of length $L/2$ is just *half* the number of clusters common to the two segments.

3. Crosses

A contour in the form of a cross of edge length $L/2$ is put on a set of lattice points (see the right panel of Fig. 1). In this geometry, there are four exterior angles of size $\gamma = 2\pi$ and another four exterior angles with $\gamma = \pi/2$, thus the corner contributions cancel out. Hence we also considered contours Γ consisting of two, three, or four crosses. In this case, there is a nonvanishing corner contribution if the number of 2π angles differs from the number of $\pi/2$ angles. The resulting corner contribution for these different configurations is indicated in the caption of Fig. 2. To use the geometric approach for this setup, we calculate $\langle N_\Gamma \rangle$ in different geometries, for example, comparing the four crosses geometry (rightmost panel in Fig. 2) with the setup of having four independent crosses (leftmost panel in Fig. 2). Making use of the possible combinations of the geometries we obtain several independent estimates of the corner contribution. As a result of this improved averaging, the crosses setup is usually found to yield the smallest relative error of the geometries considered here.

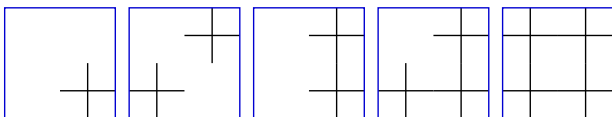


FIG. 2. (Color online) Contours consisting of different numbers of crosses. The value of the geometrical factor, A_Γ in Eq. (12), is given for these geometries from left to right by 0, 0, $-1/8$, $-1/6$, and $-1/4$, respectively, where the values have been normalized to the area of one cross.

4. Line segments at a free boundary

In our last geometry, the sample of size $L \times L$ has two free boundaries, whereas periodic boundary conditions are used in the other direction. The contour is chosen to be a line segment of length $L/2$ lying at the free boundary. In this case, the magnetization profile is not homogeneous and the Cardy-Peschel formula does not work. Instead, the logarithmically divergent corner contribution follows from the properties of the boundary condition changing operator and its prefactor has been calculated in terms of the Coulomb gas parameter as [34,35]

$$b = \frac{\beta_s}{8} = \frac{1 - 4/g}{\pi} \sin(\pi g/2). \quad (15)$$

B. Fortuin-Kasteleyn clusters

We first considered the scaling of the corner contributions for the FK clusters, which are directly encoding the critical behavior of the model. For the case of the (sheared) square, cf. Fig. 1, for each sample configuration of the Potts spins or bonds of the random-cluster representation, respectively, we averaged over 10^3 different positions of the contour. For each lattice size up to $L = 1024$, we computed the corner contribution according to the geometric approach as discussed above in Sec. III A 1. The size dependence of the prefactor $b = b(L)$ was obtained by logarithmic two-point fits to the data at sizes $L/2$ and L , then linearly extrapolated to the limit $1/L \rightarrow 0$, cf. Ref. [12].

The results of this analysis for the cases $Q = 0.5, 2, 3$, and 4 are shown in Fig. 3 for the two used cluster definitions as a function of the opening angle, γ . (For $Q = 1$ a similar figure can be found in Ref. [12].) In each panel, the conformal prediction of Eq. (14) is also indicated by a full line. For not too small values of $\gamma \gtrsim 0.1$, the finite size corrections are small and the different estimates for $b(L)$ agree well with the conformal prediction. With decreasing γ the finite-size corrections increase continuously, but for each γ the values extrapolated for $L \rightarrow \infty$ are in good agreement with the conformal prediction. We also estimated the parameter $\beta(Q)$ of Eq. (11) by dividing the extrapolated prefactor by the angle dependent factor A_Γ in Eq. (14). The results are shown in the insets of Fig. 3. For $Q \leq 3$, the estimates for $\beta(Q)$ are independent of the opening angle γ and within statistical errors the averages are in excellent agreement with the conformal conjecture. For the limiting case $Q = 4$, on the other hand, where the transition is about to become discontinuous, the agreement is less convincing. This, however, is not surprising as strong additional logarithmic corrections are expected for this case [33]. Hence, significantly larger system sizes beyond the reach of today's computational resources would be required to clearly resolve the asymptotic behavior. The extrapolated values of $\beta(Q)$ for squares are summarized in Table I.

We repeated the calculation of the corner contribution for the other two types of contours, namely the line segments (in the bulk) and the crosses, cf. Fig. 1. For the former, we averaged over all horizontal and vertical positions of the segments on the lattice. For the crosses, we averaged either over all positions (for $L = 64$) or over 10^4 random positions (for $L \geq 128$) for each sample. Using the procedure discussed above, the relation

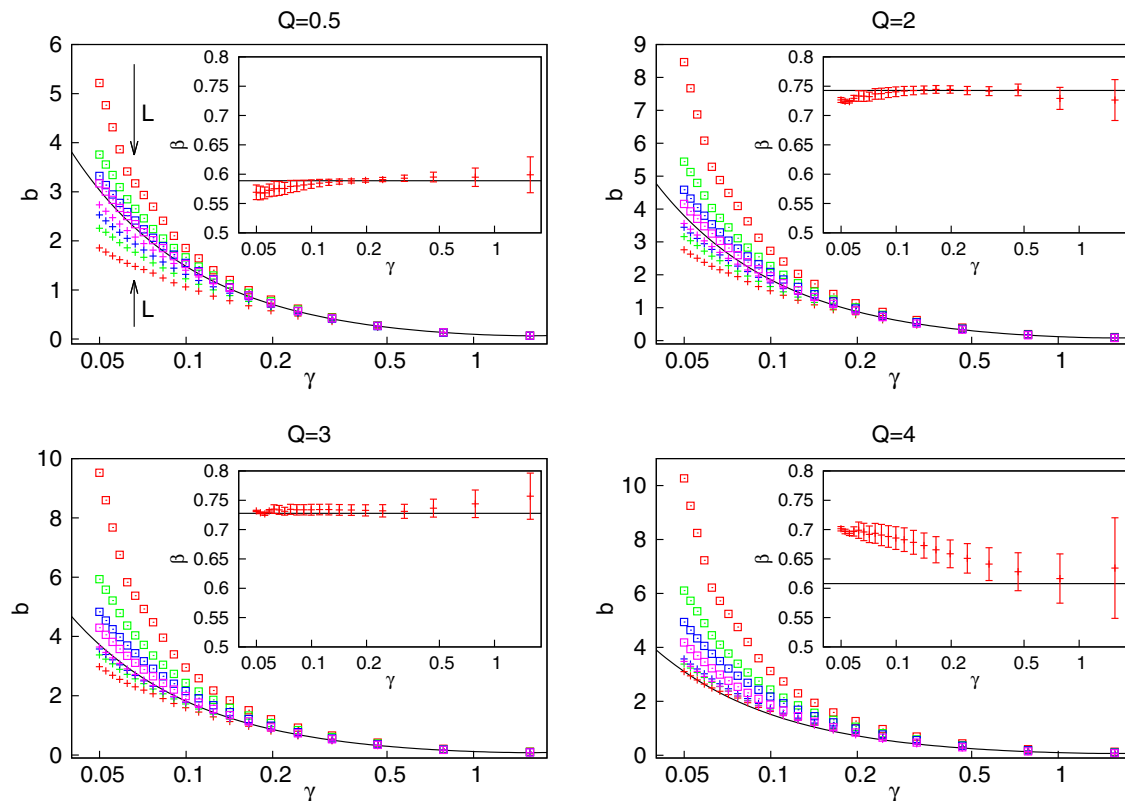


FIG. 3. (Color online) Finite-size estimates [$L = 128$ (red), 256 (green), 512 (blue), and 1024 (magenta)] of the prefactor b according to Eq. (12) of the corner contribution to the FK cluster numbers with sheared squares as a function of γ for type (a) (+) (L increasing upwards) and type (b) (\square) (L increasing downwards) clusters. For larger sizes, the results are closer to the conformal result in Eq. (14) that is indicated by the full line. The insets show the ratio of the estimated prefactor b and the angle dependent factor A_Γ in Eq. (14) as a function of γ .

Eq. (12) was used to extract an estimate of β from extrapolating $b(L)$ for $1/L \rightarrow 0$ and dividing by the angular dependency A_Γ . The corresponding estimates are collected in Table I. For $Q < 4$, the estimates for the different contours agree with each other and all of them are statistically well consistent with the conformal prediction. For $Q = 4$, the estimates for β are less satisfactory which, again, is attributed to the presence of logarithmic corrections.

For the case of the line segment adjacent to a free boundary, we again averaged over all possible positions. Due to the lack of translational invariance, however, these are by a factor of L fewer than for the bulk case, leading to correspondingly less precise results. The prefactor, β_s , is estimated in the same way as for the bulk segments. The corresponding values are collected in Table III and illustrated in the right panel of Fig. 6. The conformal conjectures are shown for comparison. Again, the numerical and conformal results are in excellent agreement for all values of Q considered with the exception of $Q = 4$ where some moderate finite-size deviations are seen.

C. Spin clusters

As discussed above in Sec. II, we also considered corner contributions to the number of spin clusters crossing a specific contour Γ . In terms of the diluted Hamiltonian Eq. (13) this corresponds to the choice $p = 1$ or $J \rightarrow \infty$. As was noted previously [14,26], the (attractive) fixed point corresponding to the behavior of spin clusters is not located at $p = 1$, but at some

$p_S = p_S(Q)$. This is where the smallest scaling corrections are measured. (For $Q = 2$ an unphysical value of $p_S > 1$ is observed, but for $Q = 3$ and 4 one finds $p_S < 1$ [14,26].) In our case, however, we find only negligible scaling corrections when working directly with the spin clusters, which we analyze here for system sizes up to $L = 2048$. The more general case of arbitrary $0 < p \leq 1$ will be discussed below in Sec. III D.

For sheared squares, the resulting estimates of the size dependent prefactors for $Q = 2, 3$ and 4 are shown in Fig. 4 as a function of the angle γ . As for the FK clusters, the finite-size corrections for the two types of clusters have opposite signs, thus allowing for a more efficient extrapolation $L \rightarrow \infty$. The extrapolated values of the prefactors, which are indicated by dashed lines in Fig. 4, however, do *not* agree with the results

TABLE III. Estimates for the prefactor β_s , calculated for a line segment at a free boundary for FK clusters (upper part) and spin clusters (lower part). In both cases, the conformal predictions (for spin clusters resulting from analytical continuation of the FK results) are presented in the second row.

Q	0.5	1	2	3	4
FK	1.056(9)	1.101(20)	0.848(29)	0.462(76)	0.13(11)
CFT	1.0543	1.1027	0.8488	0.4411	0
Spin	–	0	1.080(57)	1.245(47)	0.54(18)
CFT	–	0	0.5513	0.4036	0

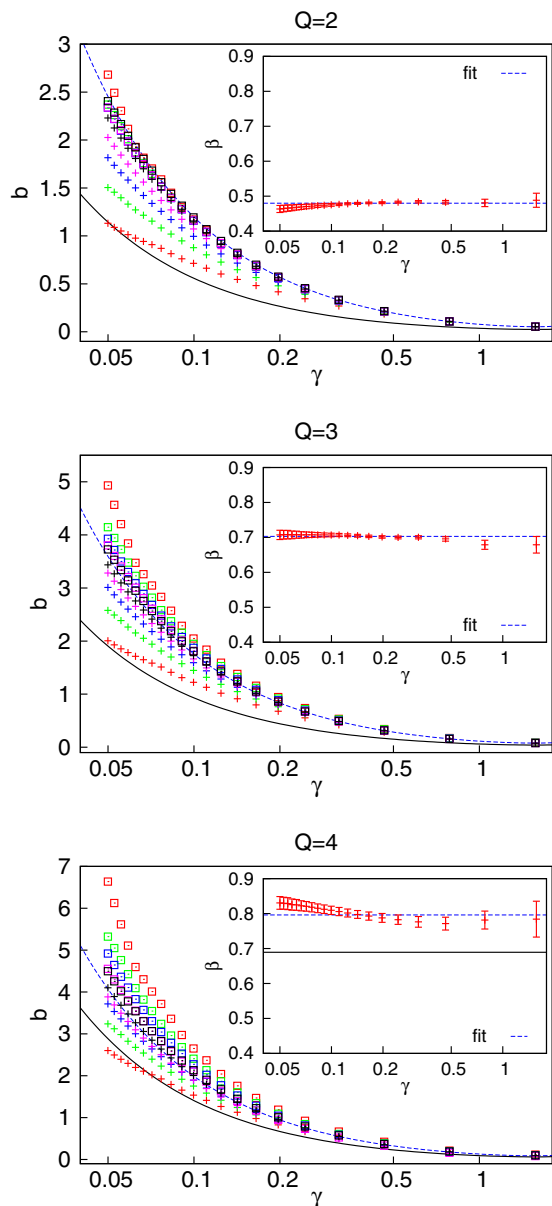


FIG. 4. (Color online) Numerical estimates for the prefactor β of the corner contribution for the spin clusters for systems up to 2048×2048 spins for sheared squares with opening angle γ . (The data for $L = 2048$ are presented in black.) The numerically extrapolated prefactors are indicated by the dashed lines, while the analytical continuation of the conformal FK results are drawn with full lines. The insets show the ratio of the estimated prefactor b and the angle dependent factor A_Γ in Eq. (14).

obtained through analytic continuation of the conformal results for FK clusters. The latter are indicated by solid lines in Fig. 4. The ratio of the extrapolated $b(Q)$ and the conformal prediction is approximately constant and has practically no angular dependence, with some deviations attributed to the presence of logarithmic corrections for the limiting case $Q = 4$. As a result, we can factorize the measured $b(Q)$ as given in Eq. (12), but its Q dependent part $\beta(Q)$, does *not* agree with the result obtained through analytic continuation of the conformal results

for FK clusters. The numerical estimates for $\beta(Q)$ are shown in the insets of Fig. 4 and summarized in Table II.

For the other geometries, in particular the line segments in the bulk and the crosses, we arrive at the same observations. The angular dependence is in perfect agreement with the conformal predictions, but the $\beta(Q)$ parameters do not agree with the results of analytical continuation. Notwithstanding these deviations, the estimates of $\beta(Q)$ for the three different geometries are in good agreement with each other, cf. the data in Table II.

Finally, we also considered the corner contributions for spin clusters and a line segment at a free boundary. As for the FK clusters, we calculated the prefactor β_s , and the estimated values are listed in Table III together with the conjectured results obtained from Eq. (15) by analytical continuation. Again, the numerical results are different from the conjectured ones, the numerical data being larger than the conjectured values by roughly a factor of Q .

D. Geometrical clusters

In the previous two sections, we have studied the bond-diluted model of Eq. (13) for two specific values of p corresponding to the fixed point of FK clusters, $p = p_{\text{FK}}$, and to spin clusters at $p = 1$. Generalizing on this, we might allow for the bond-dilution parameter p to vary between $0 < p \leq 1$ and (using the geometric approach) study the corner contribution $\langle N_\Gamma^c \rangle$ of the resulting generalized, geometrical clusters at the critical coupling K_c of the underlying random-cluster model. For the case of the Ising-like system $Q = 2$ and using crosses as contours Γ (comparing one and four crosses in Fig. 2, in which case $A_\Gamma = -1/4$), we show the results of such simulations for a range of different system sizes in Fig. 5. Here, for each sample, we averaged over at least 10^3 positions.

As is clearly seen from Fig. 5, for $p < p_{\text{FK}}$ the finite-size results converge to a limiting curve, whereas for $p \geq p_{\text{FK}}$ they grow with L . A closer inspection shows a logarithmic growth,

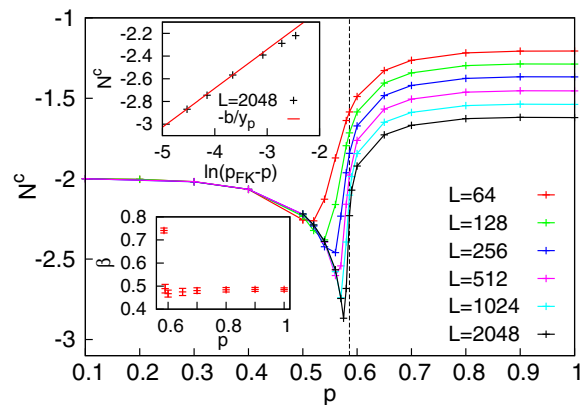


FIG. 5. (Color online) Corner contribution $\langle N_\Gamma^c \rangle$ for critical geometrical $Q = 2$ clusters with different values of the bond-dilution probability p . The FK dilution $p_{\text{FK}} = 2 - \sqrt{2}$ is indicated by the dashed line. Upper inset: $\langle N_\Gamma^c \rangle$ vs $\ln(p_{\text{FK}} - p)$ for $p < p_{\text{FK}}$ and for the largest size, $L = 2048$. The conformal prediction is shown by a straight line, see Eq. (17). Lower inset: estimated prefactor β for $p \geq p_{\text{FK}}$.

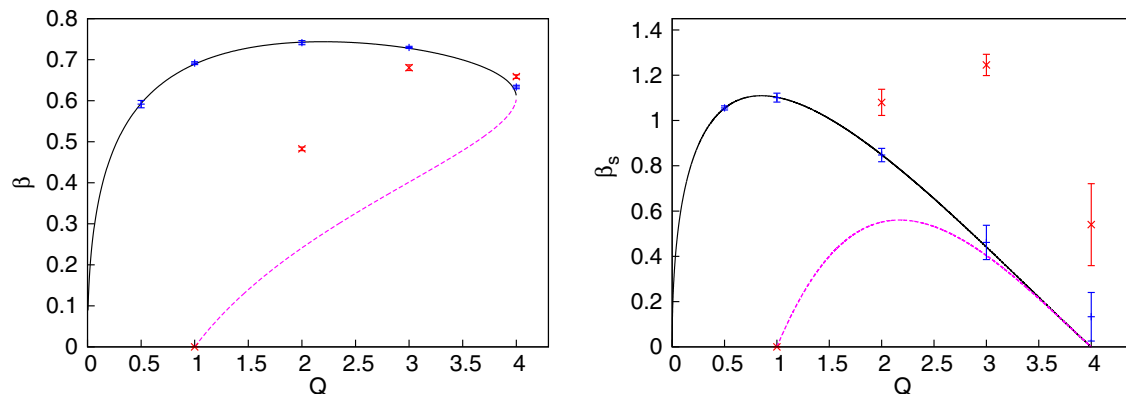


FIG. 6. (Color online) Numerical estimates for β (left) and β_s (right) for different values of Q for the FK (+) and spin (\times) clusters. The full lines represent the conformal conjectures for FK clusters and the dashed lines are the analytical continuation.

not only at the FK and at the spin cluster ($p = 1$) point, but in the complete interval as well. The prefactor of the logarithm, b , is different in (the vicinity of) the FK point, which was studied above in Sec. III B, and for $p > p_{\text{FK}}$. Performing a finite-size analysis in the latter domain, the extrapolated prefactors are found to be independent of p , at least not too close to the FK point, where the crossover effects are strong, see the lower inset of Fig. 5. This observation is in agreement with the results of the RG analysis that the critical behavior of geometrical clusters for $p > p_{\text{FK}}$ is controlled by the spin cluster fixed point and hence justifies the use of the spin-cluster limit $p = 1$ as a proxy for the spin fixed point above in Sec. III C.

For the opposite side of the FK point, $p < p_{\text{FK}}$, the numerical results in Fig. 5 indicate that the system is not critical, but has a finite correlation length, $\xi(p)$, which is divergent at $p = p_{\text{FK}}$ as $\xi(p) \sim (p_{\text{FK}} - p)^{-1/y_p}$. Here, the bond-dilution exponent at the FK fixed point, y_p , can be calculated via the Coulomb gas mapping, such that the scaling dimension $x_p = 2 - y_p$ is given by [4]

$$x_p = \frac{1}{8g}(3g - 4)(g + 4). \quad (16)$$

For the Ising model with $g = 3$, we have $x_p = 35/24$ and $y_p = 13/24$. In order to calculate the corner contribution in this noncritical regime, in the second term of the right-hand side of Eq. (9), one should replace L_Γ with $\xi(p)$, such that we obtain

$$\langle N_\Gamma^c \rangle = b \ln \xi(p) \simeq \frac{\beta}{4y_p} \ln(p_{\text{FK}} - p) + \text{const.} \quad (17)$$

In the upper inset of Fig. 5, we plot $\langle N_\Gamma^c \rangle$ as a function of $\ln(p_{\text{FK}} - p)$ and the points are approximately on a straight line with slope 1.36(2), which is compatible with the theoretical result $\beta/y_p = \frac{56}{13\pi} = 1.3712$. We have repeated the calculation for $Q = 3$ with similar conclusion, although the error in the slope is somewhat larger in this case.

IV. DISCUSSION

We have studied the corner contribution of cluster numbers in the Q -state Potts model, both for the critical Fortuin-Kasteleyn clusters and for the critical spin clusters. These investigations extend our previous studies at $Q = 1$, for

percolation, in which case $\langle N_\Gamma \rangle$ is related to the entanglement entropy of the dilute quantum Ising model [32,35,36]. We are not aware of a similar interpretation for general $Q \neq 1$, although this would be intriguing. For the FK clusters, the corner contribution is expected to be universal and has been calculated via the Cardy-Peschel formula [11]. Numerical results for different forms of the contour are in agreement with the conformal conjecture, and the parameter β agrees with the conformal results as is illustrated in the left panel of Fig. 6. For spin clusters, we follow previous studies finding that the behavior of critical spin clusters is described by the analytical continuation of the FK results [14,15,21,22] to generalize the conformal predictions for the amplitudes of the corner contributions. We find, however, that these conjectures do not agree with the numerical results. Although the angle dependence of the prefactor follows the Cardy-Peschel formula to high precision, the parameter β differs from the theoretical conjecture as is illustrated in the left panel of Fig. 6. Similar conclusions are obtained when the subsystem is a line segment at a free surface, in which case the conjectured and measured values of the parameter β_s are given in the right panel of Fig. 6.

It is known from previous investigations that the conjecture of analytical continuation of the FK results to spin clusters works on the level of the fractal dimensions and the two-point functions [14,15,21–24,26]. Similarly, the area distribution of Ising spin clusters follows this conjecture [25]. When, however, the fine structure of the conformal field theories describing critical clusters is concerned, such as for the three-point connectivities [26], the method of analytical continuation breaks down. The present results show that the universal corner contribution to critical cluster numbers also belongs to this latter class of properties. As described in Ref. [12] for the problem of percolation the universal parameter β enters into the expression of a ‘‘corner probability’’ measuring the number of clusters occupying three quadrants of a square, but have no sites in the fourth one. Also the number of clusters which have common sites with both halves of a complete line grows logarithmically with L , with a prefactor which is proportional to β . These phenomena are shown to be outside the range of validity of the simple analytical continuation conjecture.

Future directions of research extending the present study include the (annealed) site-diluted Potts model, that is assumed to feature a tricritical point in the same universality

class as the tricritical point of the diluted Potts Hamiltonian (13) discussed above [15,17,20]. In the presence of quenched impurities, it is well known that the first-order transition of the model for $Q > 4$ is softened to second order [37]. For this case, measurement of $\beta(Q)$ would give access to the central charge of the model which is of interest as conformal field theories for systems with quenched disorder are poorly understood. Finally, our investigation could be repeated for models, in which loops are defined through contour lines of surface growth models, such as the $O(N)$ model.

ACKNOWLEDGMENTS

This work has been supported by the Hungarian National Research Fund under grant Nos. OTKA K75324, K77629, and K109577. The research of IAK was supported by the European Union and the State of Hungary, co-financed by the European Social Fund in the framework of TÁMOP 4.2.4. A/2-11-1-2012-0001 “National Excellence Program.” MW acknowledges funding by the DFG under contract No. WE4425/1-1 (Emmy Noether Program).

-
- [1] R. B. Potts, *Proc. Cambridge Philos. Soc.* **48**, 106 (1952).
 [2] F. Y. Wu, *Rev. Mod. Phys.* **54**, 235 (1982).
 [3] R. J. Baxter, *J. Phys. C* **6**, L445 (1973).
 [4] B. Nienhuis in *Phase Transitions and Critical Phenomena*, edited by C. Domb and J. L. Lebowitz (Academic Press, London, 1987), Vol. 11, p. 1.
 [5] J. L. Cardy, in *Phase Transitions and Critical Phenomena*, edited by C. Domb and J. L. Lebowitz (Academic Press, London, 1987), Vol. 11, p. 55.
 [6] O. Schramm, *Israel J. Math.* **118**, 221 (2000); S. Smirnov and W. Werner, *Math. Res. Lett.* **8**, 729 (2001).
 [7] D. Stauffer and A. Aharony, *Introduction to Percolation Theory*, 2nd ed. (Taylor & Francis, London, 1992).
 [8] P. W. Kasteleyn and C. M. Fortuin, *J. Phys. Soc. Jpn.* **26**(Suppl.), 11 (1969).
 [9] A. Coniglio and W. Klein, *J. Phys. A* **13**, 2775 (1980).
 [10] C. K. Hu, *Phys. Rev. B* **29**, 5103 (1984).
 [11] J. Cardy and I. Peschel, *Nucl. Phys. B* **300**, 377 (1988).
 [12] I. A. Kovács, F. Iglói, and J. Cardy, *Phys. Rev. B* **86**, 214203 (2012).
 [13] V. S. Dotsenko and V. A. Fateev, *Nucl. Phys. B* **240**, 312 (1984).
 [14] Y. Deng, H. W. J. Blöte, and B. Nienhuis, *Phys. Rev. E* **69**, 026123 (2004).
 [15] W. Janke and A. M. J. Schakel, *Nucl. Phys. B* **700**, 385 (2004).
 [16] B. Duplantier, *J. Stat. Phys.* **110**, 691 (2003).
 [17] B. Nienhuis, A. N. Berker, E. K. Riedel, and M. Schick, *Phys. Rev. Lett.* **43**, 737 (1979).
 [18] A. L. Stella and C. Vanderzande, *Phys. Rev. Lett.* **62**, 1067 (1989).
 [19] B. Duplantier and H. Saleur, *Phys. Rev. Lett.* **63**, 2536 (1989).
 [20] X. Qian, Y. Deng, and H. W. J. Blöte, *Phys. Rev. E* **72**, 056132 (2005).
 [21] C. Vanderzande, *J. Phys. A* **25**, L75 (1992).
 [22] M. Weigel and W. Janke, *Phys. Lett. B* **639**, 373 (2006).
 [23] J. Dubail, J. L. Jacobsen, and H. Saleur, *J. Phys. A* **43**, 482002 (2010).
 [24] J. Dubail, J. L. Jacobsen, and H. Saleur, [arXiv:1010.1700](https://arxiv.org/abs/1010.1700).
 [25] J. Cardy and R. M. Ziff, *J. Stat. Phys.* **110**, 1 (2003).
 [26] G. Delfino, M. Picco, R. Santachiara, and J. Viti, *J. Stat. Mech.* (2013) **P11011**.
 [27] K. K. Murata, *J. Phys. A* **12**, 81 (1979).
 [28] A. Coniglio and F. Peruggi, *J. Phys. A* **15**, 1873 (1982).
 [29] R. H. Swendsen and J. S. Wang, *Phys. Rev. Lett.* **58**, 86 (1987).
 [30] M. Sweeny, *Phys. Rev. B* **27**, 4445 (1983).
 [31] E. M. Elçi and M. Weigel, *Phys. Rev. E* **88**, 033303 (2013).
 [32] I. A. Kovács and F. Iglói, *Europhys. Lett.* **97**, 67009 (2012).
 [33] J. L. Cardy, M. Nauenberg, and D. J. Scalapino, *Phys. Rev. B* **22**, 2560 (1980).
 [34] J. Cardy, *Phys. Rev. Lett.* **84**, 3507 (2000).
 [35] R. Yu, H. Saleur, and S. Haas, *Phys. Rev. B* **77**, 140402 (2008).
 [36] Y-C. Lin, F. Iglói, and H. Rieger, *Phys. Rev. Lett.* **99**, 147202 (2007).
 [37] M. Aizenman and J. Wehr, *Phys. Rev. Lett.* **62**, 2503 (1989); **64**, 1311(E) (1990).